Atmospheric Environment 147 (2016) 284–295

Contents lists available at ScienceDirect

Atmospheric Environment

journal homepage: www.elsevier.com/locate/atmosenv

Atmospheric inputs of organic matter to a forested watershed: Variations from storm to storm over the seasons

Lidiia Iavorivska [a, *], Elizabeth W. Boyer [a], Matthew P. Miller [b], Michael G. Brown [a], Terrie Vasilopoulos [c], Jose D. Fuentes [d], Christopher J. Duffy [e]

[a] Department of Ecosystem Science and Management, The Pennsylvania State University, University Park, PA 16802, USA
[b] U.S. Geological Survey, Utah Water Science Center, West Valley City, UT 84119, USA
[c] Department of Anesthesiology, University of Florida, Gainesville, FL 32610, USA
[d] Department of Meteorology, The Pennsylvania State University, University Park, PA 16802, USA
[e] Department of Civil and Environmental Engineering, The Pennsylvania State University, University Park, PA 16802, USA

HIGHLIGHTS

- We sampled 90 storm events of various meteorological conditions covering all climatic seasons at a continental rural site.
- We measured dissolved organic carbon (DOC) concentration and quality in precipitation, and calculated the seasonal averages.
- Summer and spring storms had higher wet atmospheric DOC deposition and more optically active organic matter than winter.
- Factors linked to storm properties, emission sources, and atmospheric composition helped explain temporal variations in DOC.
- Our observations (provided as supplement) may be useful in modeling of atmospheric chemistry and in ecosystem studies.

ARTICLE INFO

Article history:
Received 18 July 2016
Received in revised form
1 October 2016
Accepted 4 October 2016
Available online 6 October 2016

Keywords:
Precipitation
Organic matter
Dissolved organic carbon
Temporal variation
Seasonal
Critical zone observatory

ABSTRACT

The objectives of this study were to determine the quantity and chemical composition of precipitation inputs of dissolved organic carbon (DOC) to a forested watershed; and to characterize the associated temporal variability. We sampled most precipitation that occurred from May 2012 through August 2013 at the Susquehanna Shale Hills Critical Zone Observatory (Pennsylvania, USA). Sub-event precipitation samples (159) were collected sequentially during 90 events; covering various types of synoptic meteorological conditions in all climatic seasons. Precipitation DOC concentrations and rates of wet atmospheric DOC deposition were highly variable from storm to storm, ranging from 0.3 to 5.6 mg C L^{-1} and from 0.5 to 32.8 mg C m^{-2} h^{-1}, respectively. Seasonally, storms in spring and summer had higher concentrations of DOC and more optically active organic matter than in winter. Higher DOC concentrations resulted from weather types that favor air advection, where cold frontal systems, on average, delivered more than warm/stationary fronts and northeasters. A mixed modeling statistical approach revealed that factors related to storm properties, emission sources, and to the chemical composition of the atmosphere could explain more than 60% of the storm to storm variability in DOC concentrations. This study provided observations on changes in dissolved organic matter that can be useful in modeling of atmospheric oxidative chemistry, exploring relationships between organics and other elements of precipitation chemistry, and in considering temporal changes in ecosystem nutrient balances and microbial activity.

1. Introduction

Atmospheric organic matter stems from emissions from multiple biogenic and anthropogenic sources, such as vegetation, incomplete combustion of fossil fuels, biomass burning, and sea-spray (Goldstein and Galbally, 2007; Heald et al., 2008). Wet atmospheric deposition via precipitation is the primary pathway for removal of organic matter from the atmosphere (Hallquist et al., 2009; Jurado et al., 2008; Kanakidou et al., 2005). Both the

* Corresponding author.
E-mail address: lui100@psu.edu (L. Iavorivska).

http://dx.doi.org/10.1016/j.atmosenv.2016.10.002
1352-2310/

concentration, or quantity, and the chemical composition, or quality, of organics in precipitation are a reflection of sources, transport, and chemical transformations of organic matter in the atmosphere (Decesari et al., 2007; Graber and Rudich, 2006). Dissolved organic carbon (DOC) is typically used as a measure of the total dissolved organic matter (DOM) present in precipitation and other natural waters (Thurman, 1985). Precipitation contains a heterogeneous mixture of organic carbon compounds having varying molecular weights, reactivity and solubility (Altieri et al., 2009; Mead et al., 2013; Seaton et al., 2013). Studies by Fahey et al. (2005) and Pan et al. (2010) suggest that a large fraction (76–94%) of the carbon in precipitation is in the organic form. It is recognized that precipitation can supply bioavailable organic compounds to landscapes (Avery et al., 2003; Seitzinger and Sanders, 1999) and can influence multiple ecosystem functions (Kanakidou et al., 2012; Mladenov et al., 2012). Observations of DOC concentrations in precipitation are sparse worldwide (Iavorivska et al., 2016). It has only recently been established that DOC in precipitation is significant in the global carbon budget, accounting for a portion of the missing carbon sink over the land and oceans (Willey et al., 2000).

Concentrations of DOC in precipitation can span several orders of magnitude from storm to storm (Coelho et al., 2008; Sakugawa et al., 1993; Willey et al., 2009); and events differ markedly in terms of DOC quality (Kieber et al., 2006; Muller et al., 2008; Santos et al., 2009). Climatic factors have been invoked to explain variability in DOC concentration and quality from storm to storm; including precipitation depth and duration, synoptic weather pattern, wind speed, and antecedent conditions such as dry periods (Germer et al., 2007; Jordan et al., 1995; Yan and Kim, 2012). Several studies found a strong negative relationship between DOC concentration and precipitation depth (Heartsill-Scalley et al., 2007; Kawamura et al., 2001; Santos et al., 2013). Comparably, several studies found a negative relationship between precipitation depth and metrics of DOC quality, characterizing the light-absorbing or chromophoric fractions (Balla et al., 2014; Kieber et al., 2006; Santos et al., 2013). However, other studies found no relationship between DOC concentration and precipitation depth (Eklund et al., 1997; Likens et al., 1983; Pena et al., 2002), highlighting that the relationships can vary in strength and are inconsistent among locations. DOC quality in precipitation is affected by the extent of mixing in the atmospheric boundary layer; where low wind speeds that promote stagnant air and accumulation of organic carbon emissions are associated with higher quantities of humic-like substances, which are major components of DOC in precipitation (Balla et al., 2014; Muller et al., 2008). Further, storms with a high convective component had significantly higher humic-like DOC fractions compared to stratiform events (Muller et al., 2008).

Research at critical zone observatory watersheds aims to understand coupled physical, chemical, and biological processes shaping Earth's surface (Brantley et al., 2016; NSF-CZO, 2016). At the Susquehanna Shale Hills Critical Zone Observatory (SSHCZO) in central Pennsylvania (USA), recent research has focused on aspects of inorganic and organic carbon cycling in the watershed (Andrews et al., 2011; Jin et al., 2014; Yu et al., 2014). Questions remain about the magnitude of organic carbon delivered to the watershed via precipitation, and its potential importance in atmospheric and terrestrial biogeochemical processes. The objectives of this study were to determine the quantity and the quality of precipitation DOC inputs to the SSHCZO watershed; and to characterize the associated temporal variability. We hypothesized that multiple factors drive variability of DOC concentrations in precipitation among the storm events; which we explored by considering relationships between DOC, storm properties, meteorological conditions, and chemical composition of air and precipitation.

2. Methods

2.1. Sampling site

The temperate, continental study site is located in central Pennsylvania (Fig. 1) in the Appalachian Forest ecoregion of the eastern United States. The precipitation sampling site (40°66.6′ N, 77°90.4′ W) is situated in a clearing at the top of the Shale Hills subwatershed; a small headwater basin (0.08 km^2) that is continuously forested; which in turn is nested within the larger Shaver's Creek watershed of the SSHCZO. The minimally disturbed monitoring location is representative of background atmospheric conditions affected by large, upwind regional sources. Potential local sources of anthropogenic emissions in the region include a few small farms and vehicular emissions from county roads.

2.2. Precipitation and atmospheric characteristics

At the SSHCZO study site, precipitation depth was recorded at 10-min intervals (Arthur, 2016) using an Ott Pluvio 2 weighing bucket rain gage (Hach Company, Loveland, CO, USA), which is one of the gage types approved for use by the National Atmospheric Deposition Program (NADP-NTN, 2015a). Precipitation depth is measured at 15-min intervals at another location 4 km away; at site PA42 of the National Atmospheric Deposition Program (NADP-NTN, 2015b). Data from site PA42 were used to fill in periods of missing precipitation data, which were mostly attributed to power outages. Precipitation at the sampling site is similar in volume to the nearby PA42 site; computed as 0.948 multiplied by the observed precipitation depth at site PA42 based on a regression relationship developed using 2 years of contemporary monitoring data from both sites ($R^2 = 0.94$).

We sampled precipitation at the SSHCZO site during 90 storms that occurred between May 14, 2012 and August 31, 2013. This period of 1.3 years covered a range of seasonal and storm conditions. Precipitation was sampled for chemical analyses during storms using an Eigenbrodt automated precipitation collector (model NSA 181/S), situated 1.5 m above the ground in a large forest clearing at the top of the watershed (Fig. 1) and 5 m away from the precipitation gage. Sample bottles are made of high-density polyethylene and were rigorously cleaned prior to sampling. They were soaked in a 10% solution of hydrochloric acid for at least an hour, with two subsequent 24-h soaks in reverse osmosis treated water and one 24-h soak in deionized water, and then air-dried in a closed container. All sampling surfaces of the precipitation collector were cleaned between sample retrievals with deionized water and dried with lint-free laboratory wipes.

Sequential samples of precipitation were collected during wet periods only according to pre-programed regular time intervals. Once triggered by a rainfall sensor, the collector lid retracted and precipitation flowed through a 500 cm^2 collection orifice funnel, and a rotating manifold delivered the sample to a bottle opening. The collector housed eight 1-L bottles (20 mm of precipitation each), which were filled in two independent cycles (four bottles per cycle). Each cycle proceeded for 18.5 h according to a following scheme: first bottle – 30 min from an onset of the event; second, third and fourth bottles – for 6-h intervals. The second cycle started after the sensor was triggered again. The bottle openings were fitted tightly against a plate, which prevented evaporation. In the wintertime, the sensor and the lid were heated to allow for the snow samples to be collected the same way as rain. Precipitation samples were retrieved from the sampler after the end of storm events.

The individual sub-event precipitation samples were collected at regular time intervals within a storm event and then the samples

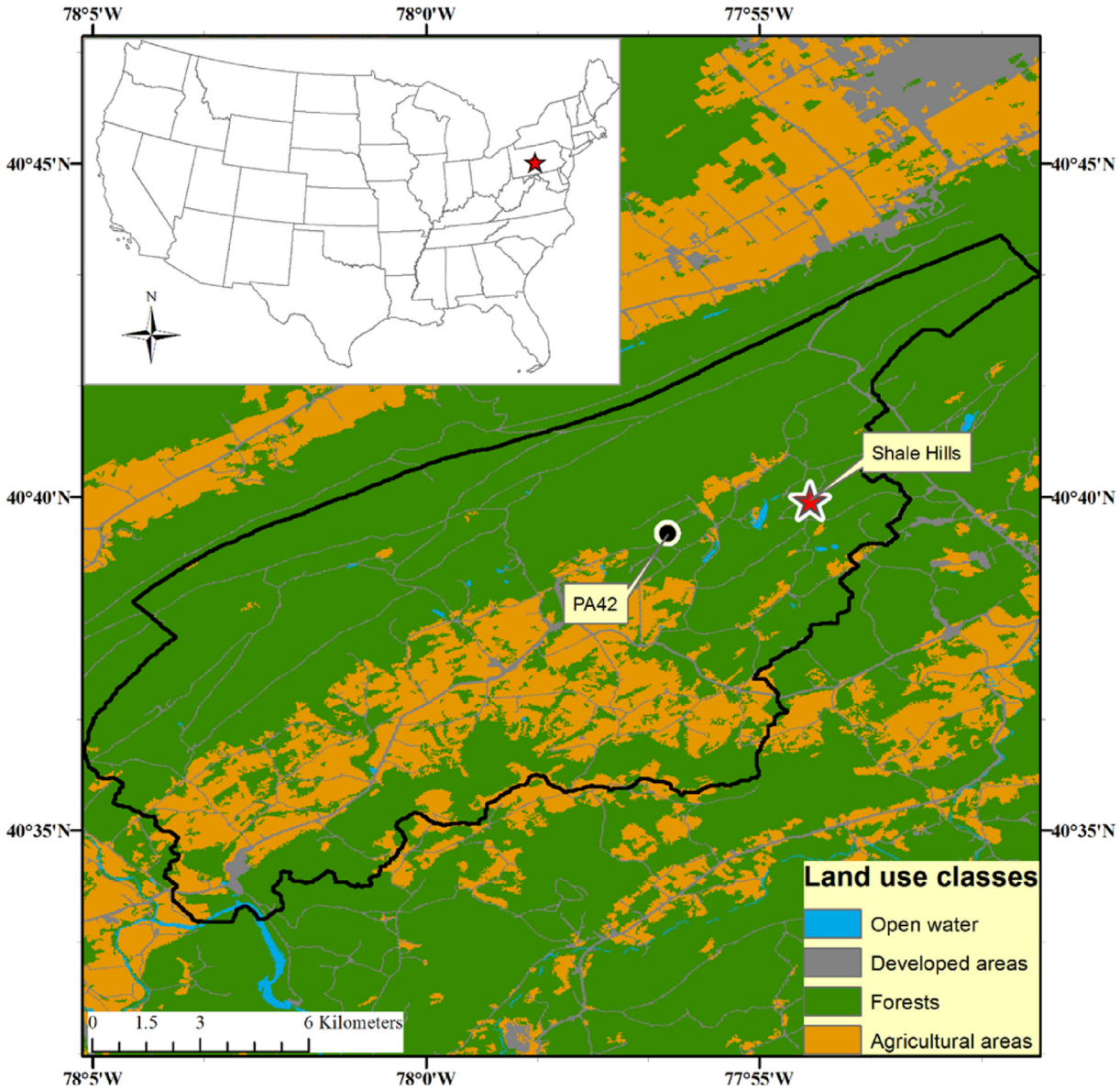

Fig. 1. The study took place within the Shaver's Creek watershed (164 km^2, black boundary from Guo, 2010) of the Susquehanna Shale Hills Critical Zone Observatory in central Pennsylvania (USA). Precipitation was sampled in a forest clearing in the Shale Hills sub-watershed (star). Auxiliary precipitation data were also obtained from the nearby site PA42 of the National Atmospheric Deposition Program (circle).

were separated by storm events. There is a lack of consensus in the literature regarding the basis for separation. Often, events are separated based on a defined minimum inter-event time (MIT), which is the duration of a break in rainfall between two back-to-back precipitation events, and it can range from 15 min to 24 h in different studies depending on intended data application and research questions (Dunkerley, 2008). For this study using MIT criterion alone seemed artificial, since we aimed to examine how changing meteorological conditions influence the delivery of constituents with precipitation. Consequently, we chose to separate the events based on a combination of MIT and information from surface weather maps. The samples of continuous precipitation were assigned to one event if they were collected less than 12 h apart and belonged to the same distinctive synoptic weather system that caused precipitation at the sampling site. Also, the samples were assigned to separate events if they originated from different systems, even when only 6 h apart (which is a duration of one sampling interval).

The antecedent depth of precipitation (mm) and the fraction of precipitation due to convection (%) were computed using the Phase 2 of the North American Land Data Assimilation System Model (Xia et al., 2012). We retrieved hourly precipitation characteristics for the sampling period from the data archive (NASA-LDAS-2, 2015). The antecedent precipitation depth was calculated by summing the hourly precipitation depths preceding each sampling date/time for the geographic coordinate of the sampling site for a specified number of hours (1, 3, 12, 24, 72, 168 h). The air temperature (°C) was measured at the SSHCZO sampling site.

One of four synoptic weather patterns (or regional storm types) were assigned for each sample: 1) warm or stationary fronts; 2) cold fronts; 3) northeasters; and 4) non-frontal. These were assigned on the basis of visual examination of surface weather maps with a three-hour time step, obtained from the Weather Prediction Center Archive by the National Weather Service (NOAA-WPC, 2015). The non-frontal type was assigned to local convective events or events due to convergence that were not associated with

frontal long-range activity, and formed as a result of surface convergence along a trough or local convection during warm months. Hurricane Sandy (October 29–30, 2012) and the winter storm Nemo (February 8, 2013) were classified as northeasters.

We also considered atmospheric ozone mixing ratio data, in parts per billion on volume basis (ppbv), and their relationships to DOC in precipitation. Ambient ozone is monitored 10 km northwest of the sampling site at the PSU106 location of the U.S. Environmental Protection Agency's Clean Air Status and Trends Network. Hourly ozone concentration data for the PSU106 location were retrieved from the data repository (USEPA-CASTNET, 2015).

2.3. Organic matter in atmospheric precipitation

2.3.1. DOC determination

Precipitation samples were transported to the Department of Ecosystem Science and Management water quality laboratory at the Pennsylvania State University. Samples were kept chilled (4 °C) until processing and analysis shortly after sample collection. If there was sufficient sample volume, one aliquot was filtered through Whatman binder-free glass-fiber filters with a nominal pore size of 0.7 μm that had been combusted for 6 h in a furnace at 450 °C. Another aliquot was left unfiltered. Both aliquots were transferred to pre-combusted amber glass bottles and refrigerated at 4 °C until analysis. There was no significant difference between filtered and unfiltered samples for organic carbon, total nitrogen, or specific ultraviolet absorbance ($n = 48$, $p = 0.5362$, a rank-based non-parametric Kruskal-Wallis test). We report results for unfiltered samples as dissolved organic carbon in this paper, as it allowed for inclusion of the low volume samples.

Concentrations of dissolved organic carbon (DOC) and total dissolved nitrogen (TDN) were measured on a Shimadzu carbon analyzer (model TOC-V_{CPH} + TNM-1, which is a high-sensitivity total organic carbon model with a total nitrogen unit). DOC analyses were conducted using the high-temperature combustion technique in non-purgeable organic carbon mode, according to procedure described in Bird et al. (2003). The detection limit for DOC was 0.015 mg C L^{-1}, and for TDN 0.015 mg N L^{-1}.

Volume-weighted DOC concentrations were calculated when full-duration precipitation events were sampled. The volume-weighted concentration per precipitation event was determined as the sum of the products of constituent concentration and precipitation depth for each sub-event sample divided by the total precipitation depth for that event. Rates of wet atmospheric DOC deposition (mg C m^{-2} $hour^{-1}$) for each sub-event sample were calculated by multiplying the concentration of a constituent (mg C L^{-1}) by the depth of precipitation from the rain gage (mm) and dividing by the precipitation duration (hours).

2.3.2. Spectroscopic measurements

To characterize the quality of organic matter in precipitation, we measured optical properties using ultraviolet–visible absorbance spectroscopy, which have been widely employed as proxies for average organic matter quality characteristics (Cory et al., 2011). When there was sufficient sample volume, absorbance of the precipitation samples was measured using a Shimadzu UV–Visible Spectrophotometer UV-1800. We used a quartz cell with 1 cm path length in the wavelength range from 190 to 1100 nm at 1 nm increments, and blank corrected. The photometric accuracy of the instrument was ±0.002 absorbance units (AU).

The following indices derived from the absorbance measurements were considered: 1) Decadic and Napierian absorption coefficients at 254 nm and 300 nm; 2) specific ultraviolet absorbance at 254 nm ($SUVA_{254}$); and 3) the spectral slope ratio (S_R). In various environments these proxies have been successfully employed to relate the quality of the whole DOC mixture to its physical properties and sources without the need to resolve its detailed chemical composition (Butman et al., 2012; Cory and Kaplan, 2012; Spencer et al., 2012). Napierian coefficients (m^{-1}) are used to infer the amount of chromophoric, light-absorbing organic matter (Chin et al., 1994; Kieber et al., 2006), and were calculated as $\alpha(\lambda) = 2.303\ A(\lambda)$, where A is a decadic absorption coefficient at a reference wavelength λ (Green and Blough, 1994). $SUVA_{254}$ values are highly and positively correlated with the degree of organic matter aromaticity (Aiken and Cotsaris, 1995; Weishaar et al., 2003) and the hydrophobic organic acid fraction of organic matter (Butman et al., 2012). $SUVA_{254}$ (L mg C^{-1} m^{-1}) was calculated by dividing the decadic absorption coefficient for a respective wavelength by DOC concentration (Weishaar et al., 2003). Spectral slope ratio S_R is inversely related to average molecular weight of organic matter and the degree of photo-oxidation (Helms et al., 2008). Spectral slope ratio S_R (dimensionless) was determined as a ratio of $S_{275-295}$ to $S_{350-400}$, where $S_{275-295}$ and $S_{350-400}$ represent the slopes of the linear regression applied to the natural log-transformed absorbance spectra from 275 to 295 and 350 to 400 nm, respectively (Helms et al., 2008).

2.4. Statistical analyses

Statistical analyses were made using SAS JMP Pro 12.1.0 (SAS Institute Inc., Cary, NC, 1989–2015). The normality of distribution for all continuous variables was evaluated using a Shapiro-Wilk W test (Razali and Wah, 2011). Precipitation depth and the associated DOC concentration data were log-normally distributed. All precipitation samples had DOC concentration values that were above detection limit and thus there were no censored values to consider statistically. Given the non-normality of distribution, we used nonparametric statistical analyses to assess the significance of differences between groups of categorized variables (e.g., to assess differences among seasons, synoptic weather patterns, or filtration methods), namely the Kruskal-Wallis rank score one-way analysis of variance (Kruskal and Wallis, 1952). In cases where more than one pair of categorized means had to be compared, the Kruskal-Wallis test was followed by the Dunn All Pairs for Joint Ranks post-hoc test that controls p-values for the number of comparisons by applying the Bonferroni adjustment. The strength and direction of monotonic relationships between continuous variables was assessed by the non-parametric Kendall Tau test (Kendall, 1938). For evaluating whether test results are statistically significant, a significance level was set at alpha of 0.05.

We developed linear mixed models (Gelman and Hill, 2007; Wu, 2009) to explore factors that might best explain the variability of DOC concentrations in precipitation from storm to storm. Our dataset had a nested structure with repeated measures, where several sub-event samples were collected throughout individual storm events. For this modeling, a time sequence variable (TS#) was assigned to each sub-event sample, and an event number variable (Event#) was assigned to each storm event to represent clustering of sub-event samples within individual events. In addition to samples with missing data, the following samples were excluded from the models (total of 11 out of 159 samples): the samples with time sequence 4 and 5 due to their small number; and the two storms of the northeaster type since they are unusual weather events that are not representative of average conditions. The events had an unequal number of sub-event samples, which led to an unbalanced sampling design. Changing chemical composition of precipitation throughout the course of individual events made the observations within events non-independent of each other. The mixed modeling approach that we used accounted for the complex covariate structure of our data by addressing both the variance

shared between sub-event samples, as well as the differences between whole events (Snijders and Bosker, 1999; Wagner et al., 2006).

A range of continuous and categorical explanatory variables were considered for inclusion in the linear mixed models. These potential explanatory variables can be divided into the following categories: 1) storm characteristics (precipitation depth and duration); 2) precipitation or atmospheric chemical composition (S_R, decadic absorption coefficient at 254 nm, concentration of total dissolved nitrogen, and ozone mixing ratio); 3) meteorological variables (convective fraction, synoptic weather pattern, ambient air temperature, and climatic season); and 4) atmospheric moisture conditions (antecedent dry period, antecedent precipitation depth). All explanatory variables, except for climatic seasons, were measured at the same level as the response variable. The response variable (DOC concentration) was natural log-transformed prior to mixed modeling analysis, and the explanatory variables were left untransformed.

We first conducted an exploratory analysis to assess the potential of each variable to affect DOC concentration, by including each of them as a single explanatory variable into a model and evaluating statistical significance (see Supplementary Table S2). We then developed a set of final models to estimate ln [DOC] from various combinations of explanatory variables that were achieved by stepwise removal of non-significant explanatory variables ($p > 0.05$). Model parameters were estimated using the maximum likelihood method and explanatory variables were modeled as fixed effects. The fixed effects are parameters that are related to the whole population, rather than individual samples, and are used to estimate the response variable but are not modeled themselves (Gelman and Hill, 2007; Pinheiro and Bates, 2000). Each model was based on an unstructured repeated covariance structure, which fits all covariance parameters. Models were assessed by two metrics: 1) Model R^2 indicating the variance explained (i.e. the proportional reduction in variance of the model including independent variables compared to null model with no independent variables); and 2) Akaike's Information Criteria (where AIC = −2log-likelihood + 2 X # of model parameters), with lower values indicating greater parsimony (Buckley et al., 2003).

3. Results and discussion

3.1. Precipitation

In this temperate climatic region, the average annual precipitation is 105.3 cm per year over 35 years of observation (1980–2015) at site PA42; or 100.4 cm per year at the sampling site as extrapolated by the aforementioned regression relationship for precipitation between the sites. Total annual precipitation observed at the sampling site was 98.8 cm in 2012 and 100.5 cm in 2013; where both years were within 1% of the average at the site, suggesting that the event sampling is representative of average annual conditions. During the study period of 1.3 years, 136.6 cm of precipitation occurred. Of this, we sampled storms during 96 cm of rainfall and snowfall, constituting about 73% of the total amount of precipitation received over the sampling period. Some events were not sampled due to periods of power outages at the SSHCZO site, or they generated insufficient precipitation volumes to enable water quality analyses. Sampling occurred during typical frontal and convective weather systems as well as several unusual events. We collected 159 individual sub-event precipitation samples during storm events over the sampling period. These sub-event samples were assigned to one of 90 precipitation events that occurred across the sampling period. Due to insufficient sample volume to facilitate water quality analyses, 22 precipitation events had samples from only part of the event, while 68 events were sampled completely throughout the full duration of the storm. Information on the precipitation samples collected and associated water quality characteristics over total, annual, and seasonal time periods are summarized in Table 1.

3.2. DOC concentrations

Concentrations of DOC in all 159 sub-event precipitation samples ranged from 0.27 to 9.41 mg C L^{-1} with a median value of 1.56 mg C L^{-1} and an average value of 1.92 mg C L^{-1} (Table 1, Supplementary Table S1). The average DOC concentration in the sampling location in central Pennsylvania is comparable with values recorded at other continental locations around the world such as 1.49 mg C L^{-1} in Schauinsland, Germany and 1.35 mg C L^{-1} in K-Puszta, Hungary (Cerqueira et al., 2010), 1.83 mg C L^{-1} in Šibenik, Croatia (Orlović-Leko et al., 2009), 1.8 mg C L^{-1} in Upper Teesdale National Nature Reserve, Northern England, UK (Chapman et al., 2008), 1.8 mg C L^{-1} in Harvard Forest, Massachusetts, USA (Currie et al., 1996), and 1.91 mg C L^{-1} in Lake Calado, Amazonas, Brazil (Williams et al., 1997). Event-based volume-weighted average concentrations and deposition rates of DOC were calculated from the 68 full duration storm events that were sampled. A comparison between simple-averaged versus volume-weighted DOC concentrations for the 68 full duration events did not show

Table 1
Characteristics of precipitation samples observed in central Pennsylvania at the Susquehanna Shale Hills Critical Zone Observatory. Single asterisk denotes values averaged from the total number of sub-event samples per time period (of the 159 individual sub-event samples that were collected during storms). Double asterisk denotes volume-weighted values averaged from the complete event periods sampled per time period (of the 68 full duration storm events that were sampled). Numbers in parentheses are sample standard deviations. The 2012–2013 period is averaged over the 1.3 years of monitoring.

Time period	Sequential precipitation sub-event samples (number)*	Precipitation events sampled; complete + partial (number)*	Average sub-event precipitation DOC concentration, (mg C/L)*	Average whole-event precipitation DOC concentration, (mg C/L)**	Average sub-event atmospheric DOC deposition, (mg/m^2/hr)*	Average whole-event atmospheric DOC deposition, (mg/m^2/hr)**
2012	**79**	**37 + 10**	**2.08 (1.53)**	**2.25 (1.38)**	**8.48 (10.75)**	**9.34 (9.11)**
Spring	12	5 + 0	1.84 (1.50)	1.71 (0.96)	4.47 (3.94)	4.62 (2.39)
Summer	39	20 + 7	2.48 (1.55)	2.57 (1.38)	12.88 (13.38)	13.34 (10.24)
Fall	28	12 + 3	1.63 (1.41)	1.93 (1.47)	4.08 (4.53)	4.33 (4.28)
2013	**80**	**31 + 12**	**1.76 (1.40)**	**1.73 (1.13)**	**7.22 (10.75)**	**6.93 (8.59)**
Winter	11	5 + 2	0.76 (0.41)	0.81 (0.35)	1.25 (0.89)	1.42 (0.99)
Spring	31	12 + 5	1.93 (1.87)	2.06 (1.58)	6.39 (10.94)	7.20 (8.99)
Summer	38	14 + 5	1.91 (0.99)	1.77 (0.61)	9.64 (11.51)	8.67 (9.29)
2012–13	**159**	**68 + 22**	**1.92 (1.47)**	**2.01 (1.29)**	**7.85 (10.74)**	**8.26 (8.90)**

any statistical difference (a line of best fit Y = 0.099 + 0.99 X, $R^2 = 0.96$, $p < 0.0001$). The volume-weighted DOC concentrations for storm events ranged from 0.30 to 5.64 mg C L^{-1} with a median value of 1.69 mg C L^{-1} and an average value of 2.01 mg C L^{-1}. The whole-event deposition hourly rates ranged from 0.45 to 32.75 mg C m^{-2} $hr^{-1}$with a median value of 4.72 mg C m^{-2} hr^{-1} and are of comparable magnitude to those reported earlier for marine rainwater (Miller et al., 2008; Sempéré and Kawamura, 1996).

Seasonal dynamics of precipitation DOC concentrations have been documented in the literature for rural sites, generally having maxima in the summer or growing season (May to October) and minima in the winter, mainly due to the dynamics of biogenic and anthropogenic emission sources, and their chemical transformation in the atmosphere (Kieber et al., 2002; Likens et al., 1983; Mladenov et al., 2012; Orlović-Leko et al., 2009; Willey et al., 2000). Our results followed this pattern, with DOC concentrations in precipitation samples generally highest in summer and lowest in the winter. DOC concentrations were significantly different between these seasons (Chi-Square 21.29, degrees of freedom 3, $p < 0.0001$): summer higher than winter ($Z = -4.09$, $p = 0.0002$) and fall ($Z = 2.65$, $p = 0.047$); and spring higher than winter ($Z = -2.68$, $p = 0.044$). Events collected during the growing season had significantly higher average DOC concentrations (2.12 mg C L^{-1}) than those from the dormant season (November to April) (1.15 mg C L^{-1}) (Chi-Square 15.47, degrees of freedom 1, $p < 0.0001$). Further, wet atmospheric DOC deposition was also significantly higher in growing than in dormant season (Chi-Square 10.04, degrees of freedom 1, $p < 0.0015$), and higher in summer than in winter ($Z = -3.35$, $p = 0.0049$). No statistical difference was detected between day-time and night-time DOC concentrations in precipitation (Chi-Square 0.88, degrees of freedom 1, $p = 0.349$).

DOC concentrations in precipitation samples had an inverse correlation with precipitation depth (Fig. 2), with low concentration associated with high precipitation depths. However, at low precipitation depths the DOC concentrations can be either low or high. The fact that this negative non-linear relationship was weak but statistically significant ($R^2 = 0.20$, $p < 0.0001$) suggests that DOC is effectively removed to the surface with precipitation but it does not just follow a dilution pattern. Other factors in addition to precipitation depth can play a role, including the differences in precipitation forms (Gioda et al., 2008; Sempéré and Kawamura, 1994), as well as abundance (Heald et al., 2008) and chemical composition of organic compounds present in the atmosphere (Mullaugh et al., 2014; Sempéré and Kawamura, 1996). The correlation was statistically significant for all climatic seasons except winter, and the strength of the relationship varied by seasons (R^2 for spring 0.23, summer 0.19, and fall 0.46). Patterns similar to our results were reported by Pan et al. (2010) for sites in Northern China.

DOC concentrations varied with different synoptic weather patterns. Storms associated with cold fronts delivered higher DOC concentrations and deposition rates than warm/stationary fronts ($p < 0.0001$) and northeasters ($p < 0.05$) (Fig. 3). Other studies (Willey et al., 2000) found similar patterns for precipitation collected in Wilmington (NC, USA). The ability of mid-latitude cold frontal systems to cause an uplift of non-methane hydrocarbon species to the atmospheric boundary layer has been documented and attributed to the convective transport associated with such systems (Purvis et al., 2003). This explanation is plausible for our samples, because there was a significant positive correlation between the fraction of precipitation due to convection and DOC concentration ($p < 0.0001$, $r = 0.34$).

3.3. DOC quality

The chemical composition of DOC was measured in 146 of the 159 sub-event samples, which had sufficient volume for these analyses. We observed large variations in DOC quality within and among the seasons (Table 2). Chromophoric dissolved organic matter (CDOM) was a ubiquitous part of DOC in all collected precipitation samples, as revealed from a significant positive correlation between Napierian absorption coefficients (254 nm and 300 nm) and DOC concentration ($r = 0.60$, $p < 0.0001$). The abundance (Napierian absorption coefficients) and aromaticity ($SUVA_{254}$) of CDOM differed by climatic seasons. Absorption coefficients were significantly higher in spring than in winter ($p < 0.05$) but did not differ statistically between growing and dormant seasons. This is opposite to observations for coastal rainwater samples, in which higher amounts of CDOM occurred in winter than in spring (Santos et al., 2013) and in dormant season than in growing season (Kieber et al., 2006). $SUVA_{254}$ in winter and spring precipitation was significantly greater ($p < 0.01$ and 0.0001, respectively) than $SUVA_{254}$ in summer precipitation. This finding compares favorably to the results of Mladenov et al. (2012) for precipitation from a continental site in the Colorado mountains (USA). Higher winter and spring aromaticity could be due to the emissions of DOM from biomass burning (wood and wood pellets) for residential heating (Duarte et al., 2005; Gelencsér et al., 2003). Lower $SUVA_{254}$ values during months with increased solar activity suggest that CDOM may have been photo-oxidized, which generally

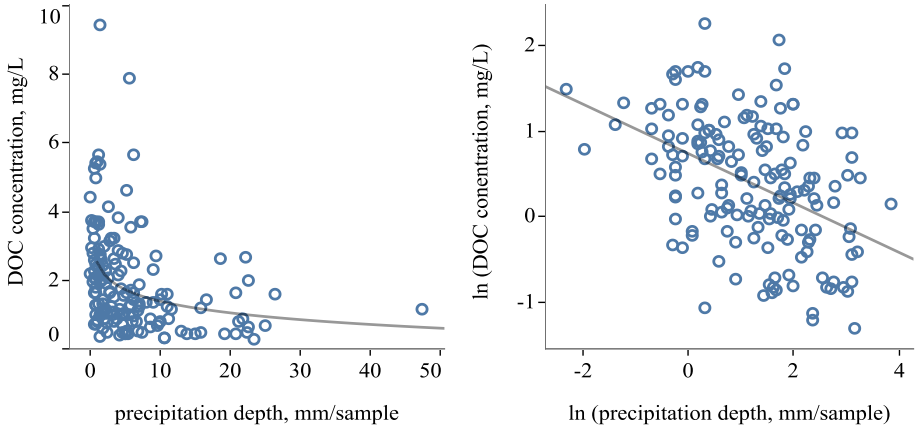

Fig. 2. The relationship between DOC concentration in precipitation (mg C/L) and depth of precipitation (mm/sample) is nonlinear: (left) non-transformed raw data with an exponential fit; (right) natural logarithm transformed data with a linear fit. The equation for both trend lines is: $\ln(y) = 0.73 - 0.29 \times \ln(x)$; $R^2 = 0.20$, $p < 0.0001$. The data are from 159 sub-event precipitation samples collected during 90 storm events occurring between May 2012 and August 2013 in central Pennsylvania.

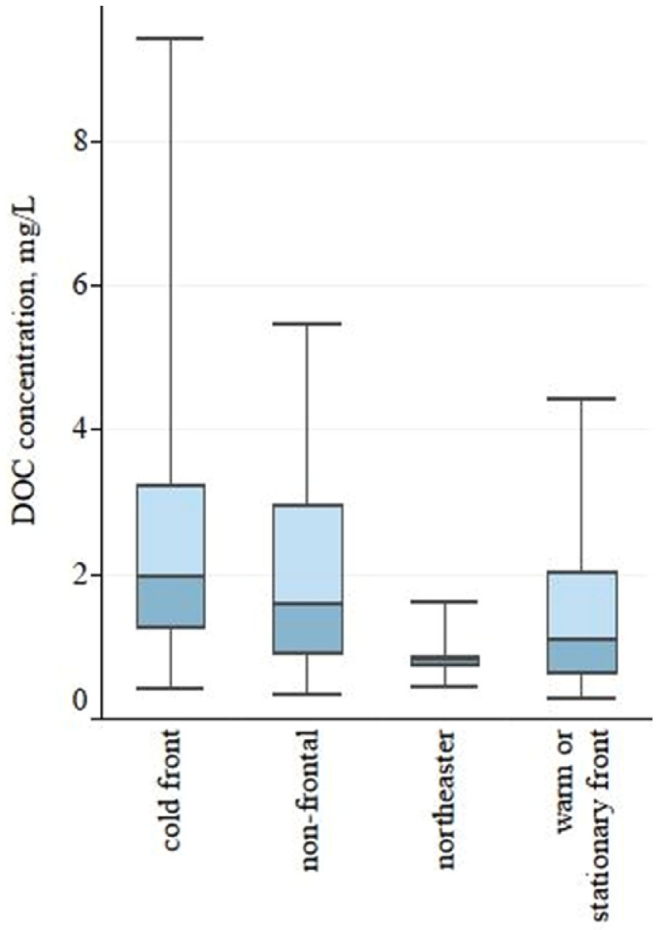

Fig. 3. DOC concentrations observed for sub-event samples during precipitation events per synoptic weather pattern. Samples were collected during storms associated with cold front systems (n = 70), non-frontal systems (n = 28), northeaster storms (n = 6), and warm or stationary front systems (n = 55). Each box represents the middle 50% of the data (between the 1st and 3rd quartile), and the horizontal line within the box represents the median value. The ends of the whiskers are minimum and maximum values.

decreases its aromaticity and molecular weight (Kieber et al., 2007). Indeed, values of S_R as a proxy for molecular weight of CDOM, though not statistically different, indicated that molecular weight had a minimum in summer and a maximum in winter. However, photo-oxidation of atmospheric DOM in summer apparently did not lead to decrease in DOC amount in precipitation since DOC concentrations were highest in the summer. This could be caused by either photo-oxidation leading to DOM being transformed to lower aromaticity compounds without its destruction to inorganic carbon and/or by higher inputs of non-chromophoric DOM.

Values of $SUVA_{254}$ showed considerable variability throughout the course of sampling ranging from 0.69 to 5.45 L mg C^{-1} m^{-1}, with an average of 2.12 L mg C^{-1} m^{-1} (Table 2 and Supplementary Table S1). Values of spectral slope ratio S_R varied from 0.49 to 2.60, with an average of 1.39 (Table 2 and Supplementary Table S1). In the precipitation samples DOC concentration displayed a significant negative correlation with $SUVA_{254}$ values ($r = -0.26$, $p < 0.0001$) and significant positive correlation with S_R ($r = 0.18$, $p < 0.001$). These relationships suggest that, on average, samples with greater concentration of DOC show lower degrees of aromaticity and lower molecular weight. This finding is opposite to what was observed in surface waters (Kang and Mitchell, 2013); where higher DOC concentrations were often caused by dissolution of high molecular weight aromatic DOM derived from terrestrial sources. In fact, the evidence presented for precipitation and aerosol samples show that DOM in atmospheric waters is dissimilar from the composition of aquatic DOM. Rainwater DOM consists of a higher proportion of aliphatic rather than aromatic structures, has lower average molecular weight, higher surface activity and a higher degree of photo-oxidation (Dinar et al., 2006; Duarte et al., 2007; Graber and Rudich, 2006; Santos et al., 2012). The differences were attributed to contrasting mechanisms of formation (biotic vs abiotic), photochemical transformations in the atmosphere, or to the overall molecular structure of the atmospheric DOM mixture.

3.4. Factors affecting variations of DOC concentration in precipitation

Results from statistical modeling revealed the direction and strength of relationships of various environmental factors with ln [DOC], with 95% confidence intervals (Supplementary Table S2). For example, positive relationships (Fig. 4) exist between precipitation ln [DOC] and: decadic absorption coefficient at 254 nm ($R^2 = 0.45$, $p < 0.0001$), total dissolved nitrogen concentration in precipitation ($R^2 = 0.38$, $p < 0.0001$), and ambient air ozone concentration ($R^2 = 0.16$, $p < 0.0001$).

Three parsimonious linear mixed models had the top R^2 and the lowest AIC values of the various combinations explored that can account for between 61% and 71% of the variability in ln [DOC] concentrations in precipitation (Table 3). The residual unexplained variance might be related to variables that did not make it to the final model but were significant on their own, such as precipitation

Table 2
Characteristics of measures of DOC quality in precipitation samples observed in central Pennsylvania, from 146 individual sub-event precipitation samples collected sequentially during storms having enough volume for these water quality analyses. Numbers in parentheses are sample standard deviations. The 2012–2013 period is averaged over the 1.3 years of monitoring.

Time period	Average $SUVA_{254}$, specific ultraviolet absorbance @ 254 nm (L mg C^{-1} m^{-1})	Average Napierian absorption coefficient @ 254 nm (m^{-1})	Average Napierian absorption coefficient @ 300 nm (m^{-1})	Average S_R, spectral slope ratio (dimensionless)
2012	**1.91 (0.71)**	**7.84 (7.43)**	**3.90 (3.88)**	**1.51 (0.47)**
Spring	2.26 (0.39)	9.52 (8.43)	4.34 (4.28)	1.60 (0.24)
Summer	1.60 (0.65)	8.50 (8.73)	4.34 (4.62)	1.61 (0.51)
Fall	2.16 (0.75)	6.14 (4.32)	3.10 (2.26)	1.31 (0.43)
2013	**2.31 (0.95)**	**8.66 (8.43)**	**4.81 (4.89)**	**1.28 (0.32)**
Winter	2.67 (0.57)	4.04 (1.98)	2.20 (0.94)	1.35 (0.32)
Spring	2.59 (0.77)	10.89 (9.34)	6.48 (5.82)	1.22 (0.37)
Summer	1.98 (1.08)	7.88 (8.12)	4.01 (4.12)	1.32 (0.25)
2012–13	**2.12 (0.86)**	**8.26 (7.94)**	**4.37 (4.44)**	**1.39 (0.41)**

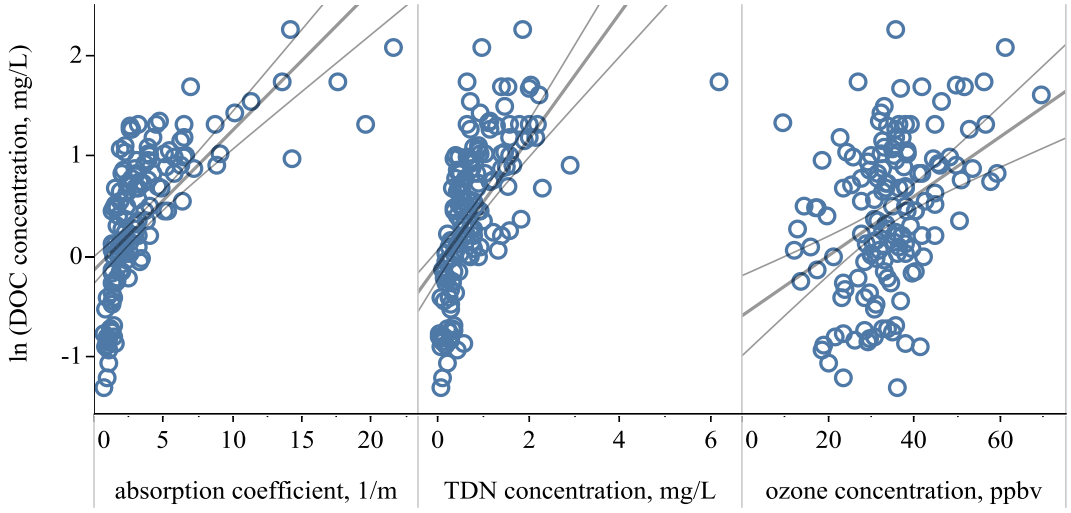

Fig. 4. Positive relationships between natural log-transformed DOC concentrations in precipitation with other chemical elements in precipitation (decadic absorption coefficient and total dissolved nitrogen concentration); and in air (ambient ozone concentration). Trend lines are displayed with 95% confidence intervals.

depth (see Supplementary Table S2). The equation to estimate ln [DOC] for each final model can be formulated from the information in Table 3, where: t (time sequence) is nested within e (storm event), and β represents regression coefficients for each explanatory variable. For example, for Model 2, $\ln(DOC)_{te} = \beta_{0e}(\text{Intercept}) + \beta_{1e}(\text{Precipitation Duration})_{te} + \beta_{2e}(\text{Antecedent Dry Period})_{te} + \beta_{3e}(\text{Total Dissolved Nitrogen})_{te} + \beta_{4e}(\text{Ozone})_{te} + \beta_{5e}(S_R)_{te} + \beta_{6e}(\text{Air Temperature})_{te} + \varepsilon_{te}$(error term). The three contrasting models are useful for generating hypotheses about potential factors that affect DOC concentrations in precipitation.

Storm characteristics were important in the observed precipitation DOC responses. The duration of precipitation was a significant explanatory variable in all three models. The negative relationship between precipitation duration and DOC concentrations in precipitation may suggest the importance of below-cloud scavenging of DOC, which can lead to a depletion of DOC sources with prolonged precipitation. The time sequence variable describing the position of sampling within a storm was not statistically significant in the final models, suggesting that within-event DOC dynamics may not contribute substantially to the overall patterns from storm to storm. The significance of antecedent dry period for predicting DOC concentrations has been previously described by Germer et al. (2007), and can be considered a proxy for the impact that a buildup of local organic carbon emissions has on precipitation composition. In otherwise identical models in terms of explanatory variables (Table 3, models 2 and 3), substituting the fraction of precipitation due to convection for the ambient air temperature produced nearly equally good models (AIC = 176–187) that explained 61–64% of the variability in ln [DOC] concentrations. The positive relationship between DOC concentration and air temperature likely points to the influence of primary emission sources (Kanakidou et al., 2005) rather than their atmospheric transformations; because laboratory and field studies demonstrate that enhanced formation of secondary oxidation products can be inversely related to air temperature (Kavouras and Stephanou, 2002; Sheehan and Bowman, 2000).

Information on the chemical composition of precipitation was also useful toward explaining the observed precipitation DOC responses. Spectral metrics related to absorbance of the samples (either decadic absorption coefficient or spectral slope ratio) that describe the quality of dissolved organics were important explanatory variables in the three models. Further, the total dissolved nitrogen concentration of precipitation was highly significant in all three models. This may be attributed to either a co-emission of organic nitrogen compounds (where globally around a third of total nitrogen in deposition is organic; Cornell et al. (2003), Neff et al. (2002)) or the incorporation of nitrogen oxides through

Table 3
Fixed effects for the linear mixed models estimating ln [DOC] concentration in precipitation from storm to storm. Model explanatory variables are: precipitation duration (hours), antecedent dry period (hours), air temperature (°C), convective fraction (dimensionless), ambient ozone mixing ratio (ppbv), precipitation concentration of total dissolved nitrogen (TDN, mg N L^{-1}), decadic absorption coefficient at 254 nm (m^{-1}), and spectral slope ratio (S_R, dimensionless). β is a parameter estimate (estimate of the term's coefficient in the model), and SE is the standard error. Statistical significance is marked as * ($p < 0.05$), ** ($p < 0.01$), *** ($p < 0.001$). The final models are significant at $p < 0.0001$, $n = 132$.

Parameter	Model 1 β (SE)	Model 2 β (SE)	Model 3 β (SE)
Intercept	−0.5163** (0.1934)	−1.173*** (0.249)	−0.889** (0.250)
Precipitation duration	−0.089** (0.028)	−0.095** (0.032)	−0.124** (0.032)
Antecedent dry period	–	0.002* (0.001)	0.002** (0.001)
TDN concentration	0.303*** (0.062)	0.455*** (0.064)	0.400*** (0.066)
Ozone concentration	–	0.011 * (0.004)	0.012* (0.005)
Absorption coefficient	0.082*** (0.013)	–	–
Spectral slope ratio	–	0.280** (0.101)	0.332** (0.105)
Air temperature	0.032*** (0.007)	0.032*** (0.007)	–
Convective fraction	–	–	0.369** (0.118)
R^2	0.71	0.64	0.61
AIC	144	176	187

atmospheric reactions with emissions of biogenic volatile organic compounds (Cape et al., 2011 and references therein).

Similarly, information on the chemical composition of the atmosphere also was related to precipitation DOC. The observed relationships between ozone, DOC concentration and metrics of DOC chemical composition may be related to atmospheric processing of organic carbon emissions. Chemical transformation of emissions can proceed via two pathways (Ervens et al., 2011; Rudich et al., 2007), both of which require oxidants (ozone, hydroxyl radical, nitrate radical) and/or solar irradiance, and can yield optically active organic species (Altieri et al., 2006; Gelencsér et al., 2003): 1) generation of secondary organic compounds with higher molecular weight and decreased water solubility through oligomerization reactions; and 2) degradation of large molecules through photo-oxidation. The latter pathway generally leads to an increase in oxidation state, and a decrease in molecular weight and aromatic content of organic compounds rendering them more soluble (Dinar et al., 2006; Fuzzi et al., 2006; Jimenez et al., 2009; Kieber et al., 2007). The increase in solubility of organic matter promotes its mixing into cloud droplets and deposition with precipitation (Ervens et al., 2011; Hallquist et al., 2009). This may contribute to the observation that compounds with lower molecular weight and aromaticity are more readily incorporated into precipitation thus contributing more to DOC concentrations.

4. Conclusions

This study is among the first to observe temporal variation of DOC quantity and quality in precipitation across a range of precipitation events and climatic seasons. Precipitation DOC varied considerably between seasons and individual events for precipitation sampled sequentially over a 1.3-year period. Seasonally, summer and spring storms had much higher amounts of DOC and optically active organic matter than winter, but DOC in winter and spring precipitation was more aromatic than in summer.

Higher DOC concentrations appear to be associated with weather types that favor air advection in such a way that cold frontal systems, on average, delivered more than warm/stationary fronts and northeasters. This may have implications for the delivery of DOC to ecosystems with precipitation in the future when changes in regional climate affect the frequency of occurrence of different weather types (Christensen et al., 2013). Similarly, rates of DOC deposition indicated that organic carbon loadings to the watershed in precipitation are highest in summer and lowest in winter.

Results from exploratory modeling suggest that precipitation DOC concentrations are affected by storm properties (e.g., characterized here by duration and convective fraction); emission sources (antecedent dry period, air temperature); and atmospheric chemical transformations (e.g., concentrations of ground-level ozone and precipitation nitrogen, as well as by spectral properties indicating molecular weight and abundance of light-absorbing organic matter). Collectively such factors explained more than 60% of the variability observed in DOC concentrations among the storm events sampled. In addition to the emission sources, there are multiple external processes related to meteorology and atmospheric dynamics that likely work in synergy to influence the quantity and chemical properties of DOC in precipitation. Further understanding of how changes in these interactions affect wet atmospheric deposition of organics in response to climate fluctuations is important for improving the predictive models of atmospheric composition (NRC, 2016). Future studies should be directed toward quantifying the suite of factors and source-receptor relationships that control inter-event variability (from storm to storm) and intra-event variability (during storms).

Our precipitation DOC measurements were made in a rural forest clearing, under long-term average precipitation conditions, representing regional background conditions in a reference watershed. It is important to note that inputs of DOC to the watershed via precipitation will be modified in the forest setting by canopy interception, canopy drip, and throughfall; further affecting concentration and composition of organic matter (Ciglasch et al., 2004). DOC concentrations measured in canopy drip and in throughfall are generally higher than DOC measured in precipitation above the canopy, with DOC becoming more enriched by leaching of soluble organic matter from plant material (Germer et al., 2007; Levia and Frost, 2003). Future work is needed to quantify carbon loadings in precipitation to watersheds over space and time, and to assess their ecological impacts, as wet atmospheric DOC deposition is an under-reported source of carbon to watersheds.

Observational data on changes in dissolved organic matter resulting from this study (provided here as Supplementary Information, Table S3) may be useful in modeling of atmospheric oxidative chemistry, exploring relationships between organics and other elements of precipitation chemistry, and in considering temporal changes in ecosystem nutrient balances and microbial activity.

Acknowledgements

This research was conducted in Penn State's Stone Valley Forest, which is managed by the Penn State's Forest Land Management Office in the College of Agricultural Sciences. The study site is the NSF-supported Susquehanna Shale Hills Critical Zone Observatory. This work was facilitated in part by National Science Foundation grants to EWB (award number 0947962) and to CJD (award number EAR 07-25019). We thank Jeff Grimm for help with calculations of antecedent precipitation depth; and Jeremy Harper and Kevin Horner for help with field sampling. Further, we thank the Pennsylvania Department of Environmental Protection for their support of our long-term monitoring of precipitation and atmospheric deposition. We appreciate the thoughtful and helpful review comments provided by Martin Risch of the US Geological Survey, 2 anonymous reviewers, and the editors.

Appendix A. Supplementary data

Supplementary data related to this article can be found at http://dx.doi.org/10.1016/j.atmosenv.2016.10.002.

References

Aiken, G., Cotsaris, E., 1995. Soil and hydrology: their effect on NOM. Am. Water Work. Assoc. J. 36–45.

Altieri, K.E., Carlton, A.G., Lim, H.-J., Turpin, B.J., Seitzinger, S.P., 2006. Evidence for oligomer formation in clouds: reactions of isoprene oxidation products. Environ. Sci. Technol. 40, 4956–4960.

Altieri, K.E., Turpin, B.J., Seitzinger, S.P., 2009. Composition of dissolved organic nitrogen in continental precipitation investigated by ultra-high resolution FT-ICR mass spectrometry. Environ. Sci. Technol. 43, 6950–6955.

Andrews, D.M., Lin, H., Zhu, Q., Jin, L., Brantley, S.L., 2011. Hot spots and hot moments of dissolved organic carbon export and soil organic carbon storage in the Shale Hills catchment. Vadose Zone J. 10, 943. http://dx.doi.org/10.2136/vzj2010.0149.

Avery, G.B.J., Willey, J.D., Kieber, R.J., Shank, G.C., Whitehead, R.F., 2003. Flux and bioavailability of Cape Fear River and rainwater dissolved organic carbon to Long Bay, southeastern United States. Glob. Biogeochem. Cycles 17, 1–6. http://dx.doi.org/10.1029/2002GB001964.

Balla, D., Papageorgiou, A., Voutsa, D., 2014. Carbonyl compounds and dissolved organic carbon in rainwater of an urban atmosphere. Environ. Sci. Pollut. Res. Int. 12062–12073. http://dx.doi.org/10.1007/s11356-014-3080-8.

Bird, S.M., Fram, M.S., Crepeau, K.L., 2003. Method of Analysis by the U. S. Geological Survey California District Sacramento Laboratory — Determination of Dissolved Organic Carbon in Water by High Temperature Catalytic Oxidation, Method

Validation, and Quality-control Practices. High Temp. 22 p.
Brantley, S.L., DiBiase, R., Russo, T., Shi, Y., Lin, H., Davis, K.J., Kaye, M., Hill, L., Kaye, J., Eissenstat, D., Hoagland, B., Dere, A.L., Neal, A.L., Brubaker, K.M., Arthur, D.K., 2016. Designing a suite of measurements to understand the critical zone. Earth Surf. Dyn. Discuss. 4, 212–235. http://dx.doi.org/10.5194/esurfd-3-1005-2015.
Buckley, Y.M., Briese, D.T., Rees, M., 2003. Demography and management of the invasive plant species Hypericum perforatum. I. Using multi-level mixed-effects models for characterizing growth, survival and fecundity in a long-term data set. J. Appl. Ecol. 40, 481–493. http://dx.doi.org/10.1046/j.1365-2664.2003.00821.x.
Butman, D., Raymond, P.A., Butler, K., Aiken, G.R., 2012. Relationships between Δ 14 C and the molecular quality of dissolved organic carbon in rivers draining to the coast from the conterminous United States. Glob. Biogeochem. Cycles 26, 1–15. http://dx.doi.org/10.1029/2012GB004361.
Cape, J.N., Cornell, S.E., Jickells, T.D., Nemitz, E., 2011. Organic nitrogen in the atmosphere — where does it come from? A review of sources and methods. Atmos. Res. 102, 30–48. http://dx.doi.org/10.1016/j.atmosres.2011.07.009.
Cerqueira, M., Pio, C.A., Legrand, M., Puxbaum, H., Kasper-Giebl, A., Afonso, J., Preunkert, S., Gelencsér, A., Fialho, P., 2010. Particulate carbon in precipitation at European background sites. J. Aerosol Sci. 41, 51–61. http://dx.doi.org/10.1016/j.jaerosci.2009.08.002.
Chapman, P.J., Clark, J.M., Reynolds, B., Adamson, J.K., 2008. The influence of organic acids in relation to acid deposition in controlling the acidity of soil and stream waters on a seasonal basis. Environ. Pollut. 151, 110–120. http://dx.doi.org/10.1016/j.envpol.2007.03.001.
Chin, Y.-P., Aiken, G.R., O'Loughlin, E., 1994. Molecular weight, polydispersity, and spectroscopic properties of aquatic humic substances. Environ. Sci. Technol. 28, 1853–1858. http://dx.doi.org/10.1021/es00060a015.
Christensen, J.H., Kumar, K.K., Aldria, E., An, S.-I., Cavalcanti, I.F.A., Castro, M. De, Dong, W., Goswami, P., Hall, A., Kanyanga, J.K., Kitoh, A., Kossin, J., Lau, N.-C., Renwick, J., Stephenson, D.B., Xie, S.-P., Zhou, T., 2013. Climate phenomena and their relevance for future regional climate change. In: Stocker, T.F., Qin, D., Plattner, G.-K., Tignor, M., Allen, S.K., Boschung, J., Nauels, A., Xia, Y., Bex, V., Midgley, P.M. (Eds.), Climate Change 2013: the Physical Science Basis. Contribution of Working Group I to the Fifth Assessment Report of the Intergovernmental Panel on Climate Change. Cambridge University Press. http://dx.doi.org/10.1017/CBO9781107415324.028, p. 62.
Ciglasch, H., Lilienfein, J., Kaiser, K., Wilcke, W., 2004. Dissolved organic matter under native Cerrado and Pinus caribaea plantations in the Brazilian savanna. Biogeochemistry 67, 157–182.
Coelho, C.H., Francisco, J.G., Nogueira, R.F.P., Campos, M.L.A.M., 2008. Dissolved organic carbon in rainwater from areas heavily impacted by sugar cane burning. Atmos. Environ. 42, 7115–7121. http://dx.doi.org/10.1016/j.atmosenv.2008.05.072.
Cornell, S.E., Jickells, T., Cape, J., Rowland, A., Duce, R.A., 2003. Organic nitrogen deposition on land and coastal environments: a review of methods and data. Atmos. Environ. 37, 2173–2191. http://dx.doi.org/10.1016/S1352-2310(03)00133-X.
Cory, R.M., Boyer, E.W., McKnight, D.M., 2011. Spectral methods to advance understanding of dissolved organic carbon dynamics in forested catchments. In: Levia, D.F., Carlyle-Moses, D., Tanaka, T. (Eds.), Forest Hydrology and Biochemistry: Synthesis of Past Research and Future Directions, Ecological Studies. Springer, Netherlands, Dordrecht, pp. 117–136. http://dx.doi.org/10.1007/978-94-007-1363-5.
Cory, R.M., Kaplan, L.A., 2012. Biological lability of streamwater fluorescent dissolved organic matter. Limnol. Oceanogr. 57, 1347–1360. http://dx.doi.org/10.4319/lo.2012.57.5.1347.
Currie, W.S., Aber, J.D., McDowell, W.H., Boone, R.D., Magill, A.H., 1996. Vertical transport of dissolved organic C and N under long-term N amendments in pine and hardwood forests. Biogeochemistry 35, 471–505.
Decesari, S., Mircea, M., Cavalli, F., Fuzzi, S., Moretti, F., Tagliavini, E., Facchini, M.C., 2007. Source attribution of water-soluble organic aerosol by nuclear magnetic resonance spectroscopy. Environ. Sci. Technol. 41, 2479–2484. http://dx.doi.org/10.1021/es061711l.
Dinar, E., Taraniuk, I., Graber, E.R., Katsman, S., Moise, T., Anttila, T., Mentel, T.F., Rudich, Y., 2006. Cloud Condensation Nuclei properties of model and atmospheric HULIS. Atmos. Chem. Phys. Discuss. 6, 2465–2482. http://dx.doi.org/10.5194/acp-6-2465-2006.
Duarte, R.M.B.O., Pio, C.A., Duarte, A.C., 2005. Spectroscopic study of the water-soluble organic matter isolated from atmospheric aerosols collected under different atmospheric conditions. Anal. Chim. Acta 530, 7–14. http://dx.doi.org/10.1016/j.aca.2004.08.049.
Duarte, R.M.B.O., Santos, E.B.H., Pio, C.A., Duarte, A.C., 2007. Comparison of structural features of water-soluble organic matter from atmospheric aerosols with those of aquatic humic substances. Atmos. Environ. 41, 8100–8113. http://dx.doi.org/10.1016/j.atmosenv.2007.06.034.
Dunkerley, D., 2008. Identifying individual rain events from pluviograph records: a review with analysis of data from an Australian dryland site. Hydrol. Process. 22, 5024–5036. http://dx.doi.org/10.1002/hyp.
Eklund, T.J., McDowell, W.H., Pringle, C.M., 1997. Seasonal variation of tropical precipitation chemistry: La Selva, Costa Rica. Atmos. Environ. 31, 3903–3910.
Ervens, B., Turpin, B.J., Weber, R.J., 2011. Secondary organic aerosol formation in cloud droplets and aqueous particles (aqSOA): a review of laboratory, field and model studies. Atmos. Chem. Phys. 11, 11069–11102. http://dx.doi.org/10.5194/acp-11-11069-2011.
Fahey, T.J., Siccama, T.G., Driscoll, C.T., Likens, G.E., Campbell, J., Johnson, C.E., Battles, J.J., Aber, J.D., Cole, J.J., Fisk, M.C., Groffman, P.M., Hamburg, S.P., Holmes, R.T., Schwarz, P.A., Yanai, R.D., 2005. The biogeochemistry of carbon at Hubbard Brook. Biogeochemistry 75, 109–176. http://dx.doi.org/10.1007/s10533-004-6321-y.
Fuzzi, S., Andreae, M.O., Huebert, B.J., Kulmala, M., Bond, T.C., Boy, M., Doherty, S.J., Guenther, A., Kanakidou, M., Kawamura, K., Kerminen, V.-M., Lohmann, U., Russell, L.M., Poschl, U., 2006. Critical assessment of the current state of scientific knowledge, terminology, and research needs concerning the role of organic aerosols in the atmosphere, climate, and global change. Atmos. Chem. Phys. 6, 2017–2038.
Gelencsér, A., Hoffer, A., Kiss, G., Tombacz, E., Kurdi, R., Bencze, L., 2003. In-situ formation of light-absorbing organic matter in cloud water. J. Atmos. Chem. 45, 25–33. http://dx.doi.org/10.1023/A:1024060428172.
Gelman, A., Hill, J., 2007. Data Analysis Using Regression and Multilevel/Hierarchical Models, first ed. Cambridge University Press. http://dx.doi.org/10.2277/0521867061.
Germer, S., Neill, C., Krusche, A.V., Neto, S.C.G., Elsenbeer, H., 2007. Seasonal and within-event dynamics of rainfall and throughfall chemistry in an open tropical rainforest in Rondônia, Brazil. Biogeochemistry 86, 155–174. http://dx.doi.org/10.1007/s10533-007-9152-9.
Gioda, A., Mayol-Bracero, O.L., Reyes-Rodriguez, G.J., Santos-Figueroa, G., Collett, J.L., 2008. Water-soluble organic and nitrogen levels in cloud and rainwater in a background marine environment under influence of different air masses. J. Atmos. Chem. 61, 85–99. http://dx.doi.org/10.1007/s10874-009-9125-6.
Goldstein, A.H., Galbally, I.E., 2007. Known and unexpected organic constituents in the earth's atmosphere. Environ. Sci. Technol. 1515–1521.
Graber, E.R., Rudich, Y., 2006. Atmospheric HULIS: how humic-like are they? A comprehensive and critical review. Atmos. Chem. Phys. 6, 729–753.
Green, S.A., Blough, N.V., 1994. Natural waters optical absorption and fluorescence of chromophoric properties dissolved organic matter in natural waters. Limnol. Oceanogr. 39, 1903–1916.
Hallquist, M., Wenger, J.C., Baltensperger, U., Rudich, Y., Simpson, D., Claeys, M., Dommen, J., Donahue, N.M., George, C., Goldstein, A.H., Hamilton, J.F., Herrmann, H., Hoffmann, T., Iinuma, Y., Jang, M., Jenkin, M.E., Jimenez, J.L., Kiendler-Scharr, A., Maenhaut, W., McFiggans, G., Mentel, T.F., Monod, A., H., P.A.S., Seinfeld, J.H., Surratt, J.D., Szmigielski, R., Wildt, J., 2009. The formation, properties and impact of secondary organic aerosol: current and emerging issues. Atmos. Chem. Phys. 9, 5155–5236.
Heald, C.L., Goldstein, A.H., Allan, J.D., Aiken, A.C., Apel, E., Atlas, E.L., Baker, A.K., Bates, T.S., Beyersdorf, A.J., Blake, D.R., Campos, T., Coe, H., Crounse, J.D., Decarlo, P.F., de Gouw, J.A., Dunlea, E.J., Flocke, F.M., Fried, A., Goldan, P., Griffin, R.J., Herndon, S.C., Holloway, J.S., Holzinger, R., Jimenez, J.L., Junkermann, W., Kuster, W.C., Lewis, A.C., Mienardi, S., Millet, D.B., Onasch, T., Polidori, A., Quinn, P.K., Riemer, D.D., Roberts, J.M., Salcedo, D., Sive, B., Swanson, A.L., Talbot, R., Warneke, C., Weber, R.J., Weibring, P., Wennberg, P.O., Worsnop, D.R., Wittig, A.E., Zhang, R., Zheng, J., Zheng, W., 2008. Total observed organic carbon (TOOC) in the atmosphere: a synthesis of North American observations. Atmos. Chem. Phys. 8, 2007–2025.
Heartsill-Scalley, T., Scatena, F.N., Estrada, C., McDowell, W.H., Lugo, A.E., 2007. Disturbance and long-term patterns of rainfall and throughfall nutrient fluxes in a subtropical wet forest in Puerto Rico. J. Hydrol. 333, 472–485. http://dx.doi.org/10.1016/j.jhydrol.2006.09.019.
Helms, J.R., Stubbins, A., Ritchie, J.D., Minor, E.C., Kieber, D.J., Mopper, K., 2008. Absorption spectral slopes and slope ratios as indicators of molecular weight, source, and photobleaching of chromophoric dissolved organic matter. Limnol. Oceanogr. 53, 955–969. http://dx.doi.org/10.4319/lo.2008.53.3.0955.
Iavorivska, L., Boyer, E.W., DeWalle, D.R., 2016. Atmospheric deposition of organic carbon via precipitation. Atmos. Environ. http://dx.doi.org/10.1016/j.atmosenv.2016.06.006.
Jimenez, J.L., Canagaratna, M.R., Donahue, N.M., Prevot, A.S.H., Zhang, Q., Kroll, J.H., DeCarlo, P.F., Allan, J.D., Coe, H., Ng, N.L., Aiken, A.C., Docherty, K.S., Ulbrich, I.M., Grieshop, A.P., Robinson, A.L., Duplissy, J., Smith, J.D., Wilson, K.R., Lanz, V.A., Hueglin, C., Sun, Y.L., Tian, J., Laaksonen, A., Raatikainen, T., Rautiainen, J., Vaattovaara, P., Ehn, M., Kulmala, M., Tomlinson, J.M., Collins, D.R., Cubison, M.J., Dunlea, E.J., Huffman, J.A., Onasch, T.B., Alfarra, M.R., Williams, P.I., Bower, K., Kondo, Y., Schneider, J., Drewnick, F., Borrmann, S., Weimer, S., Demerjian, K., Salcedo, D., Cottrell, L., Griffin, R., Takami, A., Miyoshi, T., Hatakeyama, S., Shimono, A., Sun, J.Y., Zhang, Y.M., Dzepina, K., Kimmel, J.R., Sueper, D., Jayne, J.T., Herndon, S.C., Trimborn, A.M., Williams, L.R., Wood, E.C., Middlebrook, A.M., Kolb, C.E., Baltensperger, U., Worsnop, D.R., 2009. Evolution of organic aerosols in the atmosphere. Science 326, 1525–1529. http://dx.doi.org/10.1126/science.1180353.
Jin, L., Ogrinc, N., Yesavage, T., Hasenmueller, E.A., Ma, L., Sullivan, P.L., Kaye, J., Duffy, C., Brantley, S.L., 2014. The CO_2 consumption potential during gray shale weathering: insights from the evolution of carbon isotopes in the Susquehanna Shale Hills critical zone observatory. Geochim. Cosmochim. Acta 142, 260–280. http://dx.doi.org/10.1016/j.gca.2014.07.006.
Jordan, T.E., Correll, D.L., Weller, D.E., Goff, N.M., 1995. Temporal variation in precipitation chemstry on the shore of the Chesapeake Bay. Water. Air. Soil Pollut. 83, 263–284.
Jurado, E., Dachs, J., Duarte, C.M., Simó, R., 2008. Atmospheric deposition of organic and black carbon to the global oceans. Atmos. Environ. 42, 7931–7939. http://dx.doi.org/10.1016/j.atmosenv.2008.07.029.
Kanakidou, M., Duce, R.A., Prospero, J.M., Baker, A.R., Benitez-Nelson, C.,

Dentener, F.J., Hunter, K.A., Liss, P.S., Mahowald, N., Okin, G.S., Sarin, M., Tsigaridis, K., Uematsu, M., Zamora, L.M., Zhu, T., 2012. Atmospheric fluxes of organic N and P to the global ocean. Glob. Biogeochem. Cycles 26, 1–12. http://dx.doi.org/10.1029/2011GB004277.

Kanakidou, M., Seinfeld, J.H., Pandis, S.N., Barnes, I., Dentener, F.J., Facchini, M.C., Van Dingenen, R., Ervens, B., Nenes, A., Nielsen, C.J., Swietlicki, E., Putaud, J.P., Balkanski, Y., Fuzzi, S., Horth, J., Moortgat, G.K., Winterhalter, R., Myhre, C.E.L., Tsigaridis, K., Vignati, E., Stephanou, E.G., Wilson, J., 2005. Organic aerosol and global climate modelling: a review. Atmos. Chem. Phys. 5, 1053–1123. http://dx.doi.org/10.5194/acp-5-1053-2005.

Kang, P.-G., Mitchell, M.J., 2013. Bioavailability and size-fraction of dissolved organic carbon, nitrogen, and sulfur at the Arbutus Lake watershed, Adirondack Mountains, NY. Biogeochemistry 115, 213–234. http://dx.doi.org/10.1007/s10533-013-9829-1.

Kavouras, I.G., Stephanou, E.G., 2002. Direct evidence of atmospheric secondary organic aerosol formation in forest atmosphere through heteromolecular nucleation. Environ. Sci. Technol. 36, 5083–5091. http://dx.doi.org/10.1021/es025811c.

Kawamura, K., Steinberg, S., Ng, L., Kaplan, I.R., 2001. Wet deposition of low molecular weight mono- and di-carboxylic acids, aldehydes and inorganic species in Los Angeles. Atmos. Environ. 35, 3917–3926. http://dx.doi.org/10.1016/S1352-2310(01)00207-2.

Kendall, M.G., 1938. A new measure of rank correlation. Biometrika 30, 81–93. http://dx.doi.org/10.2307/2336325.

Kieber, R.J., Peake, B., Willey, J.D., Avery, G.B.J., 2002. Dissolved organic carbon and organic acids in coastal New Zealand rainwater. Atmos. Environ. 36, 3557–3563. http://dx.doi.org/10.1016/S1352-2310(02)00273-X.

Kieber, R.J., Whitehead, R.F., Reid, S.N., Willey, J.D., Seaton, P.J., 2006. Chromophoric dissolved organic matter (CDOM) in rainwater, Southeastern North Carolina, USA. J. Atmos. Chem. 54, 21–41. http://dx.doi.org/10.1007/s10874-005-9008-4.

Kieber, R.J., Willey, J.D., Whitehead, R.F., Reid, S.N., 2007. Photobleaching of chromophoric dissolved organic matter (CDOM) in rainwater. J. Atmos. Chem. 58, 219–235. http://dx.doi.org/10.1007/s10874-007-9089-3.

Kruskal, W.H., Wallis, A.W., 1952. Use of ranks in one-criterion variance analysis. J. Am. Stat. Assoc. 47, 583–621. http://dx.doi.org/10.1080/01621459.1952.10483441.

Levia, D., Frost, E.E., 2003. A review and evaluation of stemflow literature in the hydrologic and biogeochemical cycles of forested and agricultural ecosystems. J. Hydrol. 274, 1–29.

Likens, G.E., Edgerton, E.S., Galloway, J.N., 1983. The composition and deposition of organic carbon in precipitation. Tellus B 35, 16–24.

Mead, R.N., Mullaugh, K.M., Avery, G.B.J., Kieber, R.J., Willey, J.D., Podgorski, D.C., 2013. Insights into dissolved organic matter complexity in rainwater from continental and coastal storms by ultrahigh resolution Fourier transform ion cyclotron resonance mass spectrometry. Atmos. Chem. Phys. 13, 4829–4838. http://dx.doi.org/10.5194/acp-13-4829-2013.

Miller, C., Willey, J.D., Kieber, R.J., 2008. Changes in rainwater composition in Wilmington, NC during tropical storm Ernesto. Atmos. Environ. 42, 846–855. http://dx.doi.org/10.1016/j.atmosenv.2007.10.023.

Mladenov, N., Williams, M.W., Schmidt, S.K., Cawley, K., 2012. Atmospheric deposition as a source of carbon and nutrients to an alpine catchment of the Colorado Rocky Mountains. Biogeosciences 9, 3337–3355. http://dx.doi.org/10.5194/bg-9-3337-2012.

Mullaugh, K.M., Byrd, J.N., Avery, G.B.J., Mead, R.N., Willey, J.D., Kieber, R.J., 2014. Characterization of carbohydrates in rainwater from the southeastern North Carolina. Chemosphere 107, 51–57. http://dx.doi.org/10.1016/j.chemosphere.2014.03.014.

Muller, C.L., Baker, A., Hutchinson, R., Fairchild, I.J., Kidd, C., 2008. Analysis of rainwater dissolved organic carbon compounds using fluorescence spectrophotometry. Atmos. Environ. 42, 8036–8045. http://dx.doi.org/10.1016/j.atmosenv.2008.06.042.

Neff, J.C., Holland, E.A., Dentener, F.J., McDowell, W.H., Russell, K.M., 2002. The origin, composition and rates of organic nitrogen deposition: a missing piece of the nitrogen cycle. Biogeochemistry 57/58, 99–136.

NRC, 2016. NRC. In: The Future of Atmospheric Chemistry Research: Remembering Past, Understanding Today, Anticipating Tomorrow. National Research Council. National Academies Press, Washington, D.C. doi:10.17226/23573.

Orlović-Leko, P., Plavšić, M., Bura-Nakić, E., Kozarac, Z., Ćosović, B., 2009. Organic matter in the bulk precipitations in Zagreb and Šibenik, Croatia. Atmos. Environ. 43, 805–811. http://dx.doi.org/10.1016/j.atmosenv.2008.11.006.

Pan, Y., Wang, Y., Xin, J., Tang, G., Song, T., Wang, Y., Li, X., Wu, F., 2010. Study on dissolved organic carbon in precipitation in Northern China. Atmos. Environ. 44, 2350–2357. http://dx.doi.org/10.1016/j.atmosenv.2010.03.033.

Pena, R.M., Garcia, S., Herrero, C., Losada, M., Vazquez, A., Lucas, T., 2002. Organic acids and aldehydes in rainwater in a northwest region of Spain. Atmos. Environ. 36, 5277–5288.

Pinheiro, J.C., Bates, D., 2000. Mixed-effects Models in S and S-PLUS, first ed. Springer New York, New York, NY. http://dx.doi.org/10.1016/j.agsy.2005.11.004.

Purvis, R.M., Lewis, A.C., Carney, R.A., McQuaid, J.B., Arnold, S.R., Methven, J., Barjat, H., Dewey, K., Kent, J., Monks, P.S., Carpenter, L.J., Brough, N., Penkett, S.A., Reeves, C.E., 2003. Rapid uplift of nonmethane hydrocarbons in a cold front over central Europe. J. Geophys. Res. Atmos. 108, 1–14. http://dx.doi.org/10.1029/2002JD002521.

Razali, N.M., Wah, Y.B., 2011. Power comparisons of shapiro-wilk, kolmogorov-smirnov, lilliefors and anderson-darling tests. J. Stat. Model. Anal. 2, 21–33. http://dx.doi.org/10.1515/bile-2015-0008.

Rudich, Y., Donahue, N.M., Mentel, T.F., 2007. Aging of organic aerosol: bridging the gap between laboratory and field studies. Annu. Rev. Phys. Chem. 58, 321–352. http://dx.doi.org/10.1146/annurev.physchem.58.032806.104432.

Sakugawa, H., Kaplan, I.R., Shepard, L.S., 1993. Measurments of H2O2, aldehydes and organic acids in Los Angeles rainwater: their sources and deposition rates. Atmos. Environ. 27, 203–219.

Santos, P.S.M., Duarte, R.M.B.O., Duarte, A.C., 2009. Absorption and fluorescence properties of rainwater during the cold season at a town in Western Portugal. J. Atmos. Chem. 62, 45–57. http://dx.doi.org/10.1007/s10874-009-9138-1.

Santos, P.S.M., Santos, E.B.H., Duarte, A.C., 2013. Seasonal and air mass trajectory effects on dissolved organic matter of bulk deposition at a coastal town in south-western Europe. Environ. Sci. Pollut. Res. Int. 20, 227–237. http://dx.doi.org/10.1007/s11356-012-0971-4.

Santos, P.S.M., Santos, E.B.H., Duarte, A.C., 2012. First spectroscopic study on the structural features of dissolved organic matter isolated from rainwater in different seasons. Sci. Total Environ. 426, 172–179. http://dx.doi.org/10.1016/j.scitotenv.2012.03.023.

Seaton, P.J., Kieber, R.J., Willey, J.D., Avery, G.B.J., Dixon, J.L., 2013. Seasonal and temporal characterization of dissolved organic matter in rainwater by proton nuclear magnetic resonance spectroscopy. Atmos. Environ. 65, 52–60. http://dx.doi.org/10.1016/j.atmosenv.2012.10.026.

Seitzinger, S.P., Sanders, R.W., 1999. Atmospheric inputs of dissolved organic nitrogen stimulate estuarine bacteria and phytoplankton. Limnol. Oceanogr. 44, 721–730.

Sempéré, R., Kawamura, K., 1996. Low molecular weight dicarboxylic acids and related polar compounds in the remote marine rain samples collected from Western Pacific. Atmos. Environ. 30, 1609–1619. http://dx.doi.org/10.1016/1352-2310(95)00436-X.

Sempéré, R., Kawamura, K., 1994. Comparative distribution of dicarboxylic acids and related polar compounds in snow, rain and aerosols from urban atmosphere. Atmos. Environ. 28, 449–459.

Sheehan, P.E., Bowman, F.M., 2000. Estimated effect of temperature on secondary organic aerosol concentrations. Environ. Sci. Technol. 35, 2129.

Snijders, T.A.B., Bosker, R.J., 1999. Multilevel Analysis: an Introduction to Basic and Advanced Multilevel Modeling, first ed. Sage Publications, London.

Spencer, R.G.M., Butler, K.D., Aiken, G.R., 2012. Dissolved organic carbon and chromophoric dissolved organic matter properties of rivers in the USA. J. Geophys. Res. 117, G03001. http://dx.doi.org/10.1029/2011JG001928.

Thurman, E.M., 1985. Organic Geochemistry of Natural Waters. Martinus Nijhoff/Dr W. Junk Publishers, Dordrecht.

Wagner, T., Hayes, D.B., Bremigan, M.T., 2006. Accounting for multilevel data structures in fisheries data using mixed models. Fisheries 31, 180–187. http://dx.doi.org/10.1577/1548-8446(2006)31.

Weishaar, J.L., Aiken, G.R., Bergamaschi, B.A., Fram, M.S., Fujii, R., Mopper, K., 2003. Evaluation of specific ultraviolet absorbance as an indicator of the chemical composition and reactivity of dissolved organic carbon. Environ. Sci. Technol. 37, 4702–4708. http://dx.doi.org/10.1021/es030360x.

Willey, J.D., Kieber, R.J., Eyman, M.S., Avery, G.B.J., 2000. Rainwater dissolved organic carbon: concentrations and global flux. Glob. Biogeochem. Cycles 14, 139–148.

Willey, J.D., Kieber, R.J., Yavari, J.R., 2009. Fe(II) in coastal rainwater: changing stability and concentrations. Aquat. Sci. 71, 144–150. http://dx.doi.org/10.1007/s00027-009-9176-4.

Williams, M.R., Fisher, T.R., Melack, J.M., 1997. Chemical composition and deposition of rain in the central Amazon, Brazil. Atmos. Environ. 31, 207–217. http://dx.doi.org/10.1016/1352-2310(96)00166-5.

Wu, L., 2009. Mixed Effects Models for Complex Data, first ed. Chapman and Hall/CRC Press.

Xia, Y., Mitchell, K., Ek, M., Sheffield, J., Cosgrove, B., Wood, E., Luo, L., Alonge, C., Wei, H., Meng, J., Livneh, B., Lettenmaier, D., Koren, V., Duan, Q., Mo, K., Fan, Y., Mocko, D., 2012. Continental-scale water and energy flux analysis and validation for the North American Land Data Assimilation System project phase 2 (NLDAS-2): 1. Intercomparison and application of model products. J. Geophys. Res. 117, 1–27. http://dx.doi.org/10.1029/2011JD016048.

Yan, G., Kim, G., 2012. Dissolved organic carbon in the precipitation of Seoul, Korea: implications for global wet depositional flux of fossil-fuel derived organic carbon. Atmos. Environ. 59, 117–124. http://dx.doi.org/10.1016/j.atmosenv.2012.05.044.

Yu, X., Duffy, C., Kaye, J., Crow, W., Bhatt, G., Shi, Y., 2014. Watershed reanalysis of water and carbon cycle models at a critical zone observatory. In: Remote Sensing of the Terrestrial Water Cycle, pp. 493–509. http://dx.doi.org/10.1002/9781118872086.ch31.

Web references

Arthur, Dan K., 2016. CZO Dataset: Shale Hills - Precipitation, Meteorology (2009-2016). Observational data from the Susquehanna Shale Hills Critical Zone Observatory. Online URL: http://criticalzone.org/shale-hills/data/dataset/4940/ (Accessed July 2016).

Guo, Qinghua, 2010. CZO Dataset: Shale Hills - Digital Elevation Model (DEM), GIS/Map Data, Land Cover, LiDAR, Soil Survey (2010). Geospatial data from the Susquehanna Shale Hills Critical Zone Observatory. Online URL: http://criticalzone.org/shale-hills/data/dataset/2570/ (Accessed July 2016).

USEPA-CASTNET, 2015. U.S. Environmental Protection Agency, Clean Air Markets

Division, Clean Air Status and Trends Network (CASTNET). Raw data on Hourly Ozone concentrations from site PSU106. Online URL: https://epa.gov/castnet/ (Accessed July 2015).

NADP, 2014. U.S. National Atmoshperhic Deposition Program, Site Selection and Installation Manual, Version 1.9. National Atmospheric Deposition Program, Champaign, Illinois, 18p. Online URL: http://nadp.sws.uiuc.edu/lib/manuals/NADP_Site_Selection_and_Installation_Manual_2014_11.pdf (Accessed January 2015).

NADP-NTN, 2015a. U.S. National Atmoshperhic Deposition Program, National Trends Network, Site Operations Manual, Version 2.3. National Atmospheric Deposition Program, Champaign, Illinois, 19p. Online URL: http://nadp.sws.uiuc.edu/lib/manuals/NTN_Operations_Manual_v_2-3.pdf (Accessed July 2016).

NADP-NTN, 2015b. U.S. National Atmoshperhic Deposition Program, National Trends Network. Data Portal for monitoring site PA42. Online URL: http://nadp.sws.uiuc.edu/data/ (Accessed April 2015).

NASA-LDAS-2, 2015. U.S. National Aeronautics and Space Administration, North American Land Data Assimilation System, Phase 2 Forcing Dataset. Online URL: http://ldas.gsfc.nasa.gov/nldas/NLDAS2forcing.php (Accessed March 2015).

NOAA-WPC, 2015. U.S. National Weather Service, Weather Prediction Center, Surface Analysis Archive. Online URL: http://www.wpc.ncep.noaa.gov/archives/web_pages/sfc/sfc_archive.php (Accessed March 2015).

NOAA-CFS 2015. U.S National Oceanic and Atmospheric Administration, National Centers for Environmental Information, Climate Forecast System, historical model data and reanalyiss repository. Online URL: https://www.ncdc.noaa.gov/data-access/model-data/model-datasets/climate-forecast-system-version2-cfsv2 (Accessed March 2015).

NSF-CZO, 2016. Critical Zone Observatories. United States National Science Foundation National Program. Online URL: http://criticalzone.org/national/infrastructure/observatories-1national/ (Accessed August 2016).